CHEMISTRY
A EUROPEAN JOURNAL

DOI: 10.1002/chem.200902925

Synthesis and Self-Aggregation of Enantiopure and Racemic Molecular Tweezers Based on the Bicyclo[3.3.1]nonane Framework

Carl-Johan Wallentin, Torbjörn Wixe, Ola F. Wendt, Karl-Erik Bergquist, and Kenneth Wärnmark*[a]

Abstract: A pair of molecular tweezers (*syn*-**4**) that consists of quinoline and pyrazine units fused to a bicyclic framework is presented. The tweezers were synthesised both as a racemic mixture (*rac*-**4**) and an enantiomerically pure form ((*R*,*R*,*R*,*R*)-**4**) starting from either racemic or enantiomerically pure bicyclo[3.3.1]nonane-2,6-dione (**3**). Homochiral dimers were observed in the solid state for *rac*-**4**. The self-association of both *rac*-**4** and (*R*,*R*,*R*,*R*)-**4** was studied in solution. A weak self-association constant in $CDCl_3$ was estimated by ^{1}H NMR spectroscopic dilution titration experiments in both cases, following several proton resonances. For this purpose, a general normalisation model for the accurate determination of association constants from multiple datasets was developed. In contrast to the solid state, no diastereomeric discrimination was observed for *rac*-**4** in solution.

Keywords: aggregation · enantioselectivity · molecular tweezers · NMR titration · supramolecular chemistry

Introduction

Since the 1960s extensive research efforts have been invested in the field of host–guest chemistry aiming for the selective binding of various substrates, using synthetic receptors.[1] One type of synthetic receptor that has emerged as a prominent host compound, due to its molecular properties and for synthetic reasons, is molecular tweezers. The term molecular tweezers first appeared in 1978 in a report by Chen and Whitlock[2] and the first preorganised pair of molecular tweezers was described by Zimmerman and Vanzyl in 1987.[3] The concept has been presented since then as an important type of synthetic receptor.[4]

According to Chen and Whitlock, molecular tweezers are typically composed of two parallel or near parallel aromatic arms connected by a tether, thus creating a concave binding pocket between the aromatic arms. Another molecular receptor with similar features is the molecular cleft. Molecular clefts are sometimes considered to be a more general class of receptor, of which the molecular tweezers are a subgroup.[4,5] However, to make a distinction might seem to be a little superfluous because the recognition event occurs in a more or less shallow cleft for both types of receptors. Molecular tweezers can in principle be divided into three groups: semirigid,[6–13] conformationally labile,[2,14–20] and conformationally controlled by hydrogen bonds or metal chelation.[21–23] The interaction that mediates the recognition process can, in addition to London dispersion forces, be based on hydrogen-bonding,[24] charge-transfer,[14] ion–π,[8,25] π–π,[1] electrostatic,[8] and coupled interactions.[26]

Most common are molecular tweezers with high symmetry, but there are some chiral examples. The source of chirality has been derived from biologically active building blocks, such as usnic acid or bile acids,[27,28] from auxiliary chiral groups[29] or chirogenic centres part of the backbone of the tweezers.[4,29,30] Examples of the latter belong to the family of semirigid tweezers and are based on the bis-Tröger's base **1** and the bis-Kagan's ether analogues **2** (Scheme 1). Both systems have been synthesised as racemates, and derivatives of **1** and **2** have been isolated as enantiomerically pure forms by chromatography.[31,32]

An attractive approach is to use an optically pure building block in the synthesis of an enantiomerically pure pair of tweezers, thus avoiding separation of enantiomers and diasteromers at the end. Such a building block is bicyclo-[3.3.1]nonane-2,6-dione (**3**), which can be effectively resolved on a semilarge scale by kinetic resolution with

[a] C.-J. Wallentin, T. Wixe, Dr. O. F. Wendt, Dr. K.-E. Bergquist, Dr. K. Wärnmark
Organic Chemistry, Department of Chemistry
Lund University
P.O. Box 124, 221 00 Lund (Sweden)
Fax: (+46) 46-2228209
E-mail: kenneth.warnmark@organic.lu.se

Supporting information for this article is available on the WWW under http://dx.doi.org/10.1002/chem.200900925.

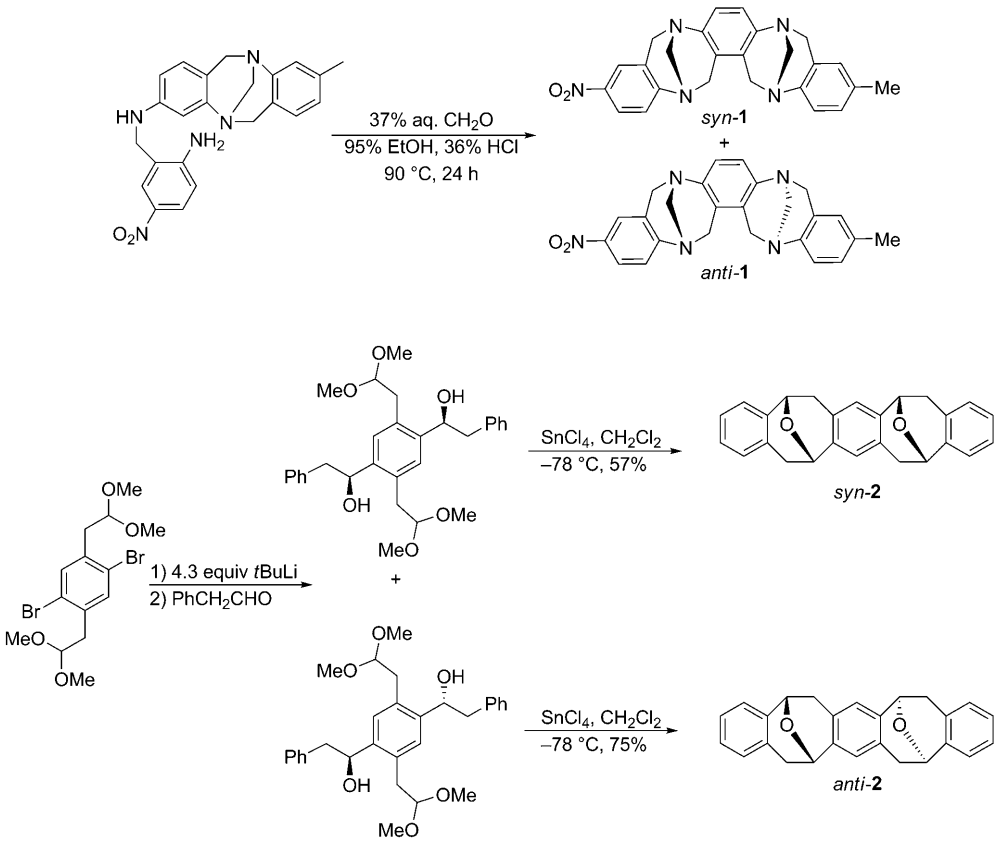

Scheme 1. Racemic molecular tweezers *syn*-**1** and *syn*-**2** based on the bis-Tröger's base and bis-Kagan's ether, respectively. The corresponding diastereomers *anti*-**1** and *anti*-**2** are also shown.

baker's yeast, according to a procedure developed by the authors.[33] Within the field of supramolecular chemistry, **3** has been used to introduce chirality into crown ethers,[34,35] as a backbone in self-complimentary hydrogen-bonding cleft molecules,[36,37] and has served as lattice-inclusion hosts.[38,39] During the course of our investigations into the development of various supramolecular architectures, we herein report on the synthesis of an enantiomerically pure pair of molecular tweezers ((*R*,*R*,*R*,*R*)-**4**) from the enantiopure bicyclo[3.3.1]nonane framework containing a pyrazine tether and quinoline arms (Scheme 2) and their self-aggregating properties in solution. We also report on the self-aggregation of the racemic pair of tweezers *rac*-**4** in solution and in the solid state.

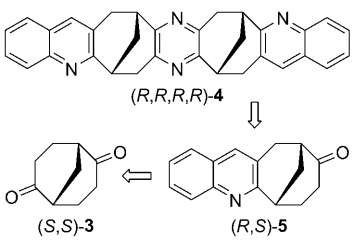

Scheme 2. Retrosynthesis of the pair of molecular tweezers (*R*,*R*,*R*,*R*)-**4** by utilising (*S*,*S*)-**3** as the starting material.

Results and Discussion

Design and retrosynthesis: The pair of tweezers **4** is based on the bicyclo[3.3.1]nonane skeleton and is C_2 symmetric with an angle between the two appending aromatic functionalities of nearly 90° (as depicted in the X-ray structure; see Figure 1). Merging two bicyclo[3.3.1]nonane moieties sets the appropriate structural features necessary for molecular tweezers. The bicycles are rather rigid, therefore giving the tweezers a preorganised conformation for guests of suitable dimensions, a favourable characteristic for a synthetic receptor as described by Zimmerman et al.[40] The inflexibility of **4** is expected to be similar to that of **1** and **2** and should hence be classified as semirigid (see above).

Pyrazine was chosen as a tether for two reasons: it allows a convergent synthesis of (*R*,*R*,*R*,*R*)-**4** from (*R*,*S*)-**5** (Scheme 2) and provides a distance of approximately 7 Å between the arms in the tweezers, which is an optimum distance for hosting aromatic guests by π–π stacking.[2] The α-aminoketone necessary for the pyrazine condensation could, in principle, be derived from ketone (*R*,*S*)-**5**, which in turn could be synthesised from (*S*,*S*)-**3** by utilising a Friedländer protocol. The choice of quinoline for the aromatic arms was attractive because there is a variety of commercially available *ortho*-aminobenzaldehydes and ketone compounds, which render the introduction of complementarity for spe-

cific guests feasible. Because the synthesis of optically pure bicyclo[3.3.1]nonane-2,6-dione is straightforward, the tweezers can be synthesised in an enantiomerically pure form on a large scale. In addition, the formation of isomers that do not have the structural characteristics of molecular tweezers, a problem common for tweezers based on the Tröger base and Kagan ether, is avoided (see Scheme 1 for examples).

Synthesis: For convenience, initial synthetic attempts towards **4** were performed on *rac*-**3**, but final yields for the enantiomerically pure synthesis agreed with the yields obtained from the racemic synthesis. Herein, we describe the enantiopure synthesis. Monoprotection of enantiopure dione (*S*,*S*)-**3**, which yields (*S*,*S*)-**6**, was achieved by diprotection followed by mono-transacetalisation with acetone in 92% yield (Scheme 3).[41] In the next step, the Friedländer condensation between (*S*,*S*)-**6** and *ortho*-aminobenzaldehyde[42] did not work under the standard conditions (i.e., using aqueous NaOH in methanol, previously successful for other bicyclo[3.3.1]nonane systems), due to low solubility.[43] However, by using a 1:1 mixture of toluene and methanol, which turned out to provide the solubility needed, with sodium methoxide or *tert*-butoxide as the base, ketal (*R*,*S*)-**7** was obtained in >99% yield. Standard acidic hydrolysis of ketal (*R*,*S*)-**7** yielded ketone (*R*,*S*)-**5** in excellent yield.

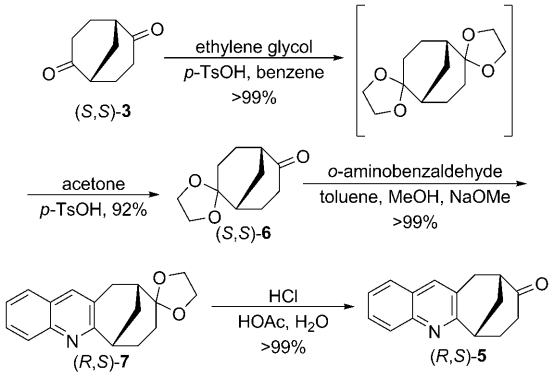

Scheme 3. High-yielding synthesis of ketone (*R*,*S*)-**5**. *p*-TsOH = *para*-toluenesulfonic acid.

Initial efforts to synthesise the intermediate required for the pyrazine condensation focussed on the synthesis of the racemic α-hydroxyimino derivative **8**, which upon subsequent reduction should give α-aminoketone derivative **9**. Surprisingly, no product was detected when standard procedures were applied that used sodium nitrite and acidic conditions. By turning to basic conditions and alkylnitrites as nitroso donors, a ring-opening reaction took place, leading to the formation of ester oxime **10** (identified by NMR spectroscopic and mass spectrometric analysis), as exemplified with isoamylnitrite in Scheme 4. This ring-opening process has been observed by others for the bicyclo[3.3.1]nonane system and has been referred to as a Beckmann fragmentation.[44] However, this reaction is formally not a fragmentation and could more accurately be denoted as a retro aza-Dieckmann condensation. The ring strain of the bicyclic structure together with the nucleophilicity of the so-formed isoamyl alkoxide explains this outcome.

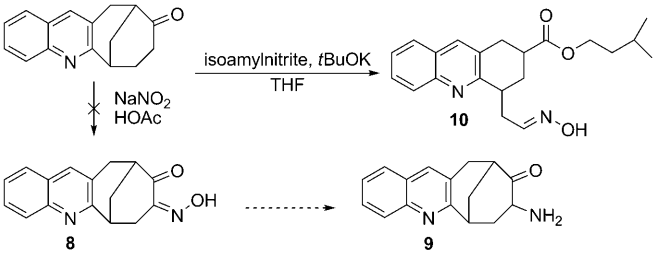

Scheme 4. Attempted synthesis of α-aminoketone **9** by using racemic material.

In an alternative approach, ketone (*R*,*S*)-**5** was brominated to give (*R*,*R*)-*exo*-**11** as the major product (Scheme 5; relative stereochemistry verified by X-ray diffraction analysis; see Figure S5 in the Supporting Information). Unexpectedly, the treatment of (*R*,*R*)-*exo*-**11** with sodium azide gave the enaminoketone (*R*,*R*)-**12** in yields that ranged from quantitative on a small scale to moderate on a larger scale. By surveying the literature, it appeared that under basic conditions the formation of enaminoketone compounds by direct loss of molecular nitrogen is rather common,[45] but continuation of the synthesis towards a pyrazine condensation was still possible. Reduction of (*R*,*R*)-**12** followed by the pyrazine condensation in one pot gave the desired tweezers (*R*,*R*,*R*,*R*)-**4** in 16% yield.

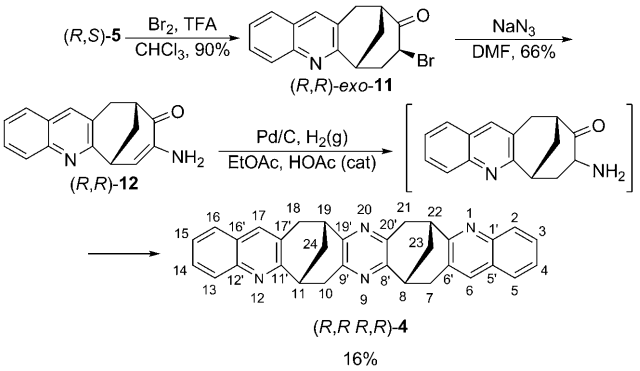

Scheme 5. Synthesis of the tweezers (*R*,*R*,*R*,*R*)-**4** from ketone (*R*,*S*)-**5**. TFA = trifluoroacetic acid.

By performing the reduction/condensation on *rac*-**12**, only one set of resonances for **4** was detected in the crude product by NMR spectroscopy. This finding implies that the condensation is diastereoselective, thus exclusively forming *rac*-**4** (*syn*-**4**) or *anti*-**4** (Scheme 6); the latter is achiral, in contrast to *anti*-**1** shown in Scheme 1. As evident from X-ray diffraction analysis (see below), only *rac*-**4** was formed, the cause for which is unclear. However, it is reasonable to

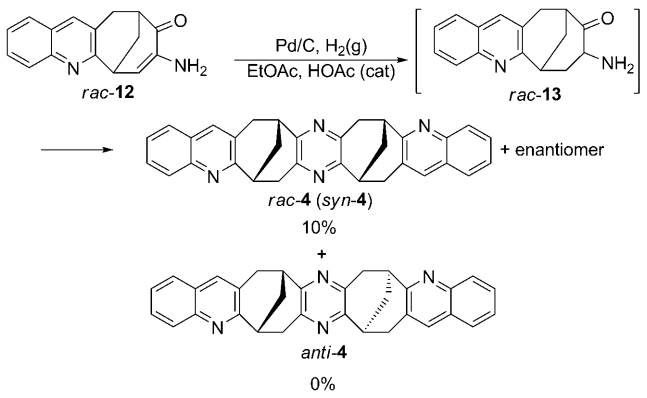

Scheme 6. Selective formation of *rac*-**4** (*syn*-**4**) from *rac*-**12**.

assume that coordination of the so-formed α-aminoketone *rac*-**13** to a palladium centre mediates the condensation, thus meaning that the selectivity observed might be due to a surface effect. Another possibility is autocatalysis: when one molecule of *rac*-**4** is formed it acts as a template by π–π stacking one molecule of *rac*-**12** or *rac*-**13** into the cavity and on the outside. Such a process is supported by the dimerisation of *rac*-**4**, observed both in the solid state and solution (see below).

X-ray diffraction analysis: Single crystals of *rac*-**4** suitable for X-ray diffraction analysis were grown from a 1:1 mixture of CH_2Cl_2 and heptane. As evident from the space group (i.e., $P2_1/n$) the crystals are racemic as well. Three individual crystals were analysed, all with the same space group, thus indicating that the bulk of the crystals is described by the reported crystal structure. The tweezers form discrete homochiral dimers in which the individual monomers are not related by symmetry, thus constituting the asymmetric unit in the unit cell (A and B; Figure 1). Consequently, the two pairs of tweezers that constitute the dimer have different conformations in the solid state. The near-to-perpendicular interpenetration of the two tweezer units is favoured by cooperative π–π stacking, which is quite commonly seen in similar systems.[11] The reason for the conformational preferences is not evident from these weak nondirectional interdimer interactions. Possibly, the presence of dichloromethane in the crystal structure imposes a conformational deviance to avoid steric congestion, thus obtaining more efficient close packing. The main planes through the pair of tweezers have an interplanar angle of 68° (plane (C-63, C-68, C-70, C-46)/(C-7, C-54, C-74, C-40)). The arms of the tweezers do not completely overlap and the torsional distortions are 71° (centroid (C-19, C-25, C-27, C-37, C-42, C-58), C-65, C-24, centroid (C-15, C-20, C-47, C-52, C-66, C-72)) and 59° (centroid (C-32, C-34, C-43, C-61, C-62, C-71), C-55, C-60, centroid (C-14, C-23, C-38, C-41, C-59, C-64)), respectively. The distances between the centroids of the tips of the pair of tweezers are 8.1 and 9.2 Å (A and B), respectively (see Figure S6 in the Supporting Information for the measurements and numbering of atoms in the X-ray structure). The small, but still significant, difference in the geometry adopted by the two pairs of tweezers clearly shows that they do have a degree of flexibility, and hence the ability to adapt the size of the cavity to a possible guest. The homochiral dimers stack along the *a* axis, in which the 2_1 screw axis generates homochiral columns and the dimers are packed by π–π stacking with 4 Å between the aromatic planes. Columns with alternating chirality then build up the complete 3D structure (Figure 2). In between the columns are dichloromethane molecules weakly hydrogen bonded to the quinoline nitrogen atoms. There are many examples of centrosymmetric enantiomer distribution in the solid state of various cleft compounds in which the packing is composed of propagating molecules with alternating handedness. However, there are also examples of significant enantiomer separation in the unit cells of similar cleft compounds.[47] The packing preferences of *rac*-**4** with respect to the chirality distribution in specific regions with a uniform sense of chirality cannot be easily explained from the presented crystal structure alone. Structures from X-ray diffraction studies of similar systems and/or from different solvents are needed to make reliable statements, something that is beyond the scope of the present report.

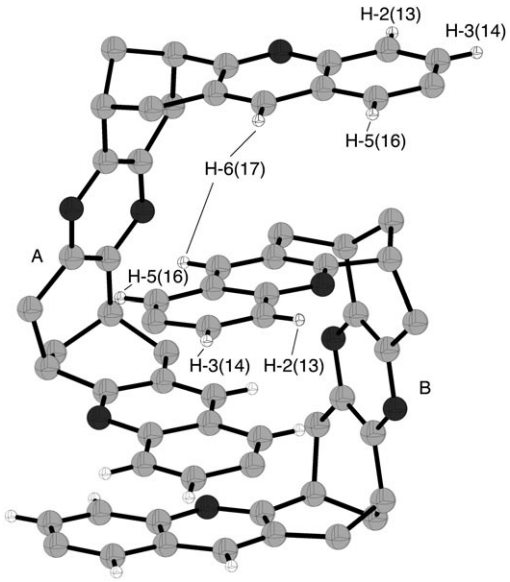

Figure 1. DIAMOND[46] representation of the X-ray data of *rac*-**4**. Two symmetrically independent molecules with the same sense of chirality (i.e., *R*,*R*,*R*,*R*) in the displayed case are associated as a dimer. Solvent molecules (CH_2Cl_2) and most of the hydrogen atoms are omitted for clarity.

Self-aggregation in solution: The X-ray crystal structure shows that the tweezers *rac*-**4** form homochiral dimers in the solid state. Thus, if present, homochiral dimerisation was expected to be the major type of aggregation for *rac*-**4** in solution as well. The three possible types of aggregation are homochiral, heterochiral, and a mixture of the two. The concentration dependence of the ^{1}H NMR spectrum of *rac*-**4** (see Figure S3 in the Supporting Information) confirmed

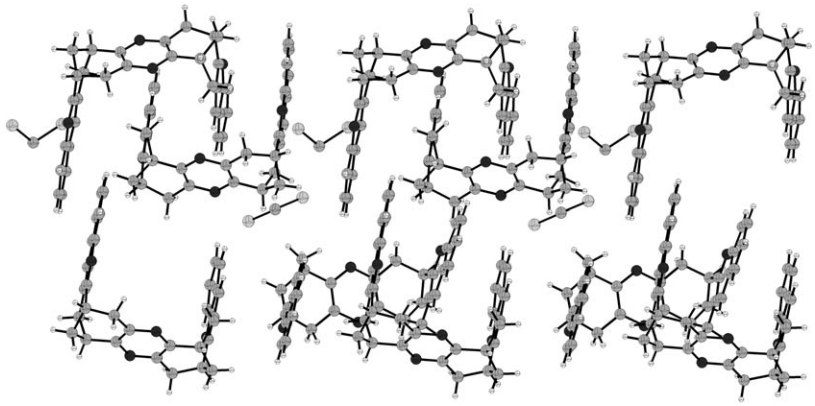

Figure 2. DIAMOND[46] representation of the X-ray data of *rac*-**4**. The formation of homochiral columns of *rac*-**4** in the solid state. Columns of a *R*,*R*,*R*,*R* sense of chirality above and *S*,*S*,*S*,*S* below. Propagation along the crystallographic *a* axis.

that the self-aggregation process also took place in $CHCl_3$. Because only one set of resonances was observed for each proton, the exchange was fast on the NMR timescale. Furthermore, repeating the titration with (*R*,*R*,*R*,*R*)-**4** gave the same collection of spectra (Figure 3), which indicated the same type of aggregation in the two cases. In addition, high-resolution mass spectrometry (ESI) strongly supports that the mode of aggregation is a dimerisation, as indicated by the dimer being the only higher aggregate observed (see Figure S16 in the Supporting Information).

In an attempt to verify the presence of potential homochiral fidelity of the dimerisation in solution as observed in the solid state, ^{1}H NMR spectra of *rac*-**4** in $CDCl_3$ were collected in the range from 273 K down to 233 K (see Figure S15 in the Supporting Information). By decreasing the rate of dimerisation so that the individual species could be detected, it would directly show if diastereomeric (e.g., heterochiral dimers) aggregates were present. However, only line broadening was observed (see Figure S15 in the Supporting Information).

In the NMR spectroscopic titration experiment, the resonance of H-6(17) (Figure 1) moves downfield as much as 1.58 ppm upon dilution of (*R*,*R*,*R*,*R*)-**4** (49.8–3.2 mM) in $CDCl_3$ (see Table 1 and Figure 3), which is in agreement with the intertwined mode of aggregation shown in the solid state. This proton is directed towards the pyrazine moiety and is also embedded by the aromatic arms of the tweezers and therefore does experience anisotropic effects more than the other protons. This behaviour means that the mode of aggregation is consistent with that as determined by X-ray diffraction analysis. This mode of aggregation is further supported by observation of an intermolecular NOE correlation between H-5(16) and H-2(13) (see Figure 1 for structure and numbering; see Figure S13.1 and S13.2 in the Supporting Information). Each atom has a chemically and magnetically identical atom generated by an internal C_2 axis within the monomeric pair of tweezers. However, when the pair of tweezers (*R*,*R*,*R*,*R*)-**4** aggregates as a dimer, each pair of atoms lose their symmetry equivalence. This behaviour means that the observed chemical shift in the ^{1}H NMR spectra for a specific proton resonance is composed of the chemical shifts of the monomeric and dimeric species, of which the latter is the arithmetic mean of the two resonances that arise from the dimeric complex (see Figure 1), each weighted against the molar fraction of the corresponding species (see the Supporting Information). The observed shift can directly be used in a common dimerisation model[48] (see the Supporting Information) to obtain an estimate of the association constant $K_{\mathrm{dim}}^{(RRRR)_2}$. Dilution titration ex-

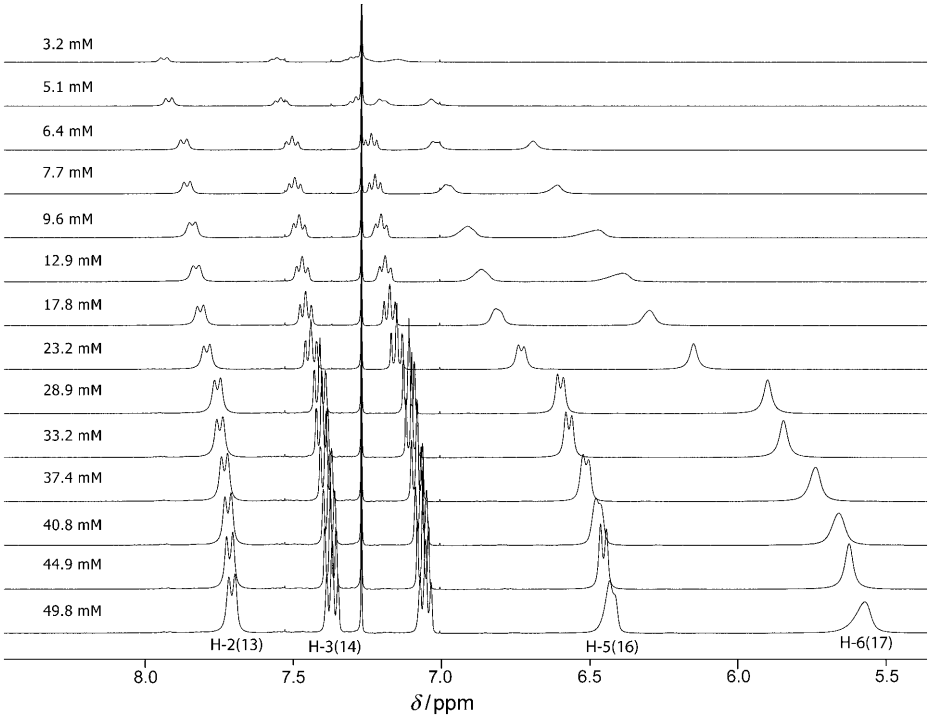

Figure 3. Part of the ^{1}H NMR (400 MHz, $CDCl_3$) spectra of (*R*,*R*,*R*,*R*)-**4** at different concentrations.

Table 1. Comparison of $\Delta\delta_{max}$, K_{dim}, and RSS for the resonances H-6(17), H-5(16), H-3(14), and H-2(13) obtained from (*R*,*R*,*R*,*R*)-**4**.[a]

Resonance	H-6(17)	H-5(16)	H-3(14)	H-2(13)
$\Delta\delta_{max}$	1.58	0.78	0.19	0.23
K_{dim} [M^{-1}]	35 ± 11	26 ± 11	25 ± 7	33 ± 10
RSS	70×10^{-3}	18×10^{-3}	0.92×10^{-3}	1.4×10^{-3}
RSS_{norm}	28×10^{-3}	30×10^{-3}	25×10^{-3}	27×10^{-3}
R^2	0.98	0.97	0.98	0.98
mean $K_{dim}^{(RRRR)_2}$ [M^{-1}]	30 ± 5[b]			

[a] Estimations of $K_{dim}^{(RRRR)_2}$ are given at a 95% confidence interval. [b] See the Supporting Information for the calculation of the mean value of K_{dim}.

periments with (*R*,*R*,*R*,*R*)-**4**, only using data from the proton that showed the largest $\Delta\delta_{max}$ value (i.e., H-6(17)) estimated $K_{dim}^{(RRRR)_2}$ to be $35\pm11\,M^{-1}$ (see Table 1 and Table S1.1 in the Supporting Information). In total, the four resonances H-6(17), H-5(16), H-3(14) and H-2(13) were used. When the dimerisation model was fitted to each of the proton resonances individually through minimisation of the residual sum of squares [RSS; defined in Eq. (1)] between δ_{obs} and δ_{calcd} values, the estimated $K_{dim}^{(RRRR)_2}$ values obtained differed between the datasets (Table 1). The quality of the fit is shown in Figure S2 and Table S1.1–1.4 in the Supporting Information.

$$RSS = \sum(\delta_{obs} - \delta_{calcd})^2 \quad (1)$$

Most frequently in the literature, association constants are estimated from data collected for one resonance only. However, the estimation of association constants based on data collected for multiple resonances will of course give a more accurate estimate of the association constant. The problem arises of how to treat the different datasets to obtain a correct value of one single association constant. One obvious way is to take the arithmetic mean of the association constant estimated from the regression analysis of each individual dataset. However, in our case, fitting the dimerisation model to each dataset from the four resonances gives values of RSS that are larger the larger $\Delta\delta_{max}$ value for that titration (Table 1). This outcome might mean that the estimated value of $K_{dim}^{(RRRR)_2}$ for each proton resonance has a different error, thus meaning that the estimated $K_{dim}^{(RRRR)_2}$ should be calculated by employing weighting of the individually estimated values of $K_{dim}^{(RRRR)_2}$ that involve, for example, $\Delta\delta_{max}$. Such weighting, proportional to $\Delta\delta_{max}$, has been employed by Hunter et al. to obtain a truer average value of the association constant.[49,50] However, care must be exercised because the normalised (relative) value of RSS [i.e., RSS_{norm}; defined in Eq. (2)] is actually almost the same for the datasets (Table 1); therefore, an arithmetic mean could be used, and thus no weighting is necessary for our datasets.

$$RSS_{norm} = \frac{RSS}{(\Delta\delta_{max})^2} \quad (2)$$

One issue that arises is how to estimate whether the values of RSS_{norm} are similar enough to allow the use of an arithmetic mean instead of a weighted mean. One way to answer this question is to see how well the theoretical relationship between RSS and $\Delta\delta_{max}$ [Eq. (2)] fits to the observed data. This fitting can be performed conveniently by using a plot of log(RSS) versus log($\Delta\delta_{max}$) of Equation (2) (see the Supporting Information). If a good linear fit is obtained, the RSS_{norm} value of all the datasets are the same and can thus be considered to have the same relative error. In our case, a good quality of the fit is obtained, which means that the four datasets have the same relative error (expressed as RSS_{norm}) and the arithmetic mean of $K_{dim}^{(RRRR)_2}$ obtained by using (*R*,*R*,*R*,*R*)-**4** was calculated to be $30\pm5\,M^{-1}$ at a 95% confidence interval (Table 1). However, global regression analyses are always preferred because the more variables that are fitted simultaneously, the more correct the fit is. By performing such a fitting of the dimerisation model to our four datasets, the value of $K_{dim}^{(RRRR)_2}$ obtained with (*R*,*R*,*R*,*R*)-**4** is estimated to be $34\pm3\,M^{-1}$ at a 95% confidence interval ($R^2=0.99$; see Table S4 in the Supporting Information). However, a global fit should not be based on the sum of RSS for each dataset because these datasets are of different scales (magnitudes) and would thus overestimate the data with the largest value of RSS. Instead the four datasets must be normalised to a common scale for reasons stated above (see the Supporting Information). The value of $K_{dim}^{(RRRR)_2}$ obtained with (*R*,*R*,*R*,*R*)-**4** was estimated to be $30\pm3\,M^{-1}$ ($R^2=0.98$; see Table S7 in the Supporting Information) at a 95% confidence interval. In our case, it is shown that the value of $K_{dim}^{(RRRR)_2}$ ($30\pm3\,M^{-1}$) from the global fitting with a normalised dataset is, as expected, in accordance with the arithmetic mean of the estimated value of $K_{dim}^{(RRRR)_2}$ from the individual regression analysis ($30\pm5\,M^{-1}$), but deviates from the estimated value of $K_{dim}^{(RRRR)_2}$ from the global fitting with non-normalised data ($34\pm3\,M^{-1}$).

It might seem a little meaningless to correct the estimated value of $K_{dim}^{(RRRR)_2}$ by a few units for a system with such a weak self-association as this system and also because the four datasets are from the same data collection, thus meaning that many types of errors are the same in the four datasets. On the other hand, the methodology for normalised global fits presented herein is an accurate way of handling multiple datasets and applies to other host–guest systems with higher association constants in which a correction might be more significant.

The dimerisation model can also be used to estimate the value of K_{dim} for *rac*-**4**. The model is only valid if there is a total presence or absence of homochiral fidelity. When fitting the dimerisation model to the ^1H NMR spectroscopic dilution titration data for *rac*-**4**, which assumes total homochiral fidelity, the so-estimated value of $K_{dim}^{(RRRR)_2}$ from a global fit of the normalised data was $56\pm1\,M^{-1}$ ($R^2=0.99$; see Table S8 in the Supporting Information) at a 95% confidence interval. This value is approximately twice the estimated value of $K_{dim}^{(RRRR)_2}$ obtained with (*R*,*R*,*R*,*R*)-**4** ($30\pm3\,M^{-1}$; see above). This discrepancy strongly indicates the absence of homochiral fidelity of *rac*-**4** in $CDCl_3$. This conclusion is further supported by the fact that when globally fit-

ting the dimerisation model to the titration data for *rac*-**4**, assuming a total absence of homochiral fidelity, $K_{dim}^{(RRRR)_2}$ was estimated to be $28\pm1\,M^{-1}$ with normalised chemical data. This leads to $K_{dim}^{RRRRSSSS}=56\pm1\,M^{-1}$ at a 95% confidence interval ($R^2=0.99$; see Table S9 in the Supporting Information) because in this case $K_{dim}^{RRRRSSSS}=2K_{dim}^{(RRRR)_2}=2K_{dim}^{(SSSS)_2}$.[51] As seen, the estimated value of $K_{dim}^{(RRRR)_2}$ obtained with *rac*-**4** is almost the same as with (*R*,*R*,*R*,*R*)-**4**, thus there is no difference between the two systems, which means that *rac*-**4** shows no measurable homochiral fidelity. Hence, our system does not exhibit the self-sorting properties observed for some chiral cleft molecules[52] in $CDCl_3$. A comparison between the fitting of the dimerisation data for (*R*,*R*,*R*,*R*)-**4** and *rac*-**4**, assuming a total absence of homochiral fidelity, based on the individual fits, is seen in Figure S2 (see also Tables S1.1–1.4 and S3.1–3.4 in the Supporting Information).

Conclusion

In summary, we have presented the synthesis of a pyrazine-tethered pair of molecular tweezers in racemic and enantiomerically pure forms. The synthesis of an enantiomerically pure pair of tweezers (*R*,*R*,*R*,*R*)-**4** starts from enantiomerically pure building blocks. This case is the first time molecular tweezers have been produced in enantiomerically pure form directly by synthesis, neither using materials from the chiral pool nor appending chiral auxiliaries. Interestingly, in the racemic synthesis only one out of two possible diastereomers was formed. In the final condensation reaction, the tweezers *rac*-**4** were exclusively formed. Homochiral fidelity is observed in the aggregation of *rac*-**4** in the solid state, but not in $CDCl_3$. To understand the aggregation of the tweezers, it should be realised that we are dealing with weak intermolecular interactions. Thus, a more or less statistical distribution of homo and hetero dimers in solution is what one would expect, which also leads to the dimerisation mode in the solid state being governed by packing forces that lead to the preference for homochiral columns. The estimated value of $K_{dim}^{(RRRR)_2}$ obtained with (*R*,*R*,*R*,*R*)-**4** and *rac*-**4** is 30 ± 3 and $28\pm1\,M^{-1}$, respectively, in $CDCl_3$. The value of $K_{dim}^{RRRRSSSS}$ was estimated to be $56\pm1\,M^{-1}$ in $CDCl_3$. All the values are at a 95% confidence interval. Self-association in similar systems, as observed by Klärner et al., which are also governed by cooperative π–π stacking interactions, was shown to give dimerisation constants on the same order of magnitude.[11] We have also demonstrated that normalised data should be used for nonlinear regression analysis involving multiple datasets, and the need for various weighting factors for different datasets can be judged from the deviation from the linear relationship between log(RSS) and $\log(\Delta\delta_{max})$. Presently, an investigation of the host characteristics of the pair of tweezers towards various guests is underway and the results will be presented in due course.

Experimental Section

General: All the chemicals were used as received from commercial suppliers. All the moisture-sensitive reactions were carried out in an atmosphere of dry nitrogen and using oven-dried glassware. Both racemic and enantiomerically pure bicyclo[3.3.1]nonane-2,6-dione were synthesised in accordance with previous reports.[33] The reaction yields are representative for both enantiomerically pure and racemic products. Column chromatography was performed on Matrex (25–70 μm) silica gel. The diameter and height of the columns are given as ($d\times h$). TLC analyses (Merck 60 F_{254} sheets) and the plates were visualised by impregnation with Seebach spot visualisation media or under UV light ($\lambda=254$ or 366 nm). Melting points were recorded on an Electrothermal IA9000 Series Digital Melting-Point apparatus and are uncorrected. Optical rotations were measured on a Perkin–Elmer 341 polarimeter at 20 °C. The ^1H and ^{13}C NMR spectra were recorded at room temperature on a Bruker DR400 spectrometer. The spectra were recorded in $CDCl_3$ and the residual solvent signals ($\delta=7.27$ and 77.16 ppm, respectively) were used as references. The assignment of (*R*,*R*,*R*,*R*)-**4** was accomplished by coupling constants, integrals, and 2D correlation experiments. Enantiomeric excess was determined with a Perkin–Elmer Autosystem XL gas chromatograph on an Alpha DEX 120 fused silica capillary column (30 m × 0.25 mm × 0.25 μm film thickness). Elemental analyses were performed by A. Kolbe of the Mikroanalytisches Laboratorium (Germany).

(+)-(1*S*,5*S*)-6,6-Ethylenedioxybicyclo[3.3.1]nonane-2-one ((*S*,*S*)-6):[41] (1*S*,5*S*)-Bicyclo[3.3.1]nonane-2,6-dione (30.0 g, 197 mmol), ethylene glycol (44 mL, 0.78 mol), and TsOH (1.1 g, 5.8 mmol) were dissolved in benzene (0.5 L) in a 1-L round-bottom flask equipped with a Dean–Stark apparatus. The reaction mixture was heated to reflux until the calculated amount of water (0.39 mmol, 7.1 mL) had been collected (typically overnight). After concentration in vacuo, acetone (340 mL) was added and the reaction mixture was stirred at 14 °C with monitoring by TLC analysis (heptane/EtOAc 7:3, R_f (**3**) = 0.26, R_f (**6**) = 0.41, R_f (diprotected) = 0.56). The reaction was quenched after 4.5 h by adding aqueous NaOH solution (1 M, ~15 mL) until pH 7–8 was reached. The reaction mixture was concentrated in vacuo and dissolved in diethyl ether. The solution was washed twice with saturated $NaHCO_3$, dried over Na_2SO_4, and concentrated in vacuo to give the crude product. Purification by flash chromatography (heptane/EtOAc 8:2, 10 × 20 cm) yielded (*S*,*S*)-**6** as a colourless oil (35.6 g, 181 mmol, 92%); $[\alpha]_D^{20}=+42$ ($c=0{,}017$ in $CHCl_3$). All the other spectroscopic data are in accordance with ref. [42].

(+)-(8*R*,12*S*)-9,9-Ethylenedioxy-8,12-methanocycloocta[5,4-*b*]quinoline ((*R*,*S*)-7): *ortho*-Aminobenzaldehyde (4.7 g, 38 mmol) and (*S*,*S*)-**6** (5.0 g, 26 mmol) were dissolved in methanol (HPLC grade) and freshly distilled toluene (1:1, 140 + 140 mL). Sodium methoxide (3.5 g, 64 mmol) was dissolved in methanol (HPLC grade; 140 mL) and added dropwise to the reaction mixture over 30 min at 0 °C. The reaction mixture was stirred at room temperature for 48 h and concentrated in vacuo. Saturated NH_4Cl aqueous solution (500 mL) was added to the obtained solid, and the reaction mixture was extracted with ethyl acetate (4 × 200 mL). The combined organic phases were washed with brine (2 × 200 mL), dried over Na_2SO_4, and concentrated in vacuo to give a brown solid crude. Purification by flash chromatography on celite (petroleum ether/EtOAc 6:4, 10 × 15 cm, $R_f=0.18$) followed by duplicate recrystallization in ethyl acetate yielded (*R*,*S*)-**7** as pale-yellow crystals (6.6 g, 24 mmol, 92%). M.p. (*rac*) 124.0–124.7 °C; m.p. (*ee* > 99%) 128.0–128.5 °C; $[\alpha]_D^{20}=+109$ ($c=0.013$ in $CHCl_3$); ^1H NMR (400 MHz, CD_2Cl_2): $\delta=7.91$ (apparent d, 1H $J=8.40$ Hz), 7.83 (s, 1H), 7.71 (apparent d, 1H $J=8.00$ Hz), 7.58 (ddd, 1H $J=1.20$, 7.00, 8.50 Hz), 7.42 (ddd, 1H $J=1.20$, 7.20, 8.60 Hz), 3.91–4.01 (m, 4H), 3.18–3.23 (m, 2H), 3.11 (ddd, 1H $J=1.20$, 7.00, 18.20 Hz), 2.26-2.31 (m, 1H), 2.18–2.20 (m, 1H), 1.95–2.07 (m, 2H), 1.79–1.84 (m, 1H,), 1.46 (ddt, 1H $J=2.00$, 4.00, 14.00 Hz), 1.18 ppm (dt, 1H $J=5.20$, 14.00 Hz); ^{13}C NMR (100 MHz, $CDCl_3$): $\delta=162.3$, 147.1, 138.6, 130.7, 128.8, 128.6, 127.8, 127.3, 125.8, 111.0, 64.9, 64.7, 37.4, 36.7, 31.5, 30.0, 29.1, 28.8 ppm; IR (KBr): $\tilde{\nu}=1491$ (m), 1618 (w), 2872 (m), 2917 (m) 2942 cm^{-1} (m); elemental analysis (%) calcd for $C_{18}H_{19}NO_2\cdot1/6\,H_2O$: C 76.03, H 6.85, N 4.93; found: C 76.28, H 7.15, N 4.83; HRMS (ESI): *m*/*z*: calcd for $C_{18}H_{20}NO_2$: 282.1494 [$M+H^+$]; found: 282.1495.

(+)-(8*R*,12*S*)-8,12-Methano-9-oxo-cycloocta[5,4-*b*]quinoline ((*R*,*S*)-5): (*R*,*S*)-**7** (8.90 g, 31.6 mmol) was dissolved in a mixture of glacial acetic acid (165 mL) and water (49 mL). Concentrated HCl (ca. 180 drops) was added and the reaction mixture was stirred at 70 °C for 3 h. The reaction mixture was cooled on an ice bath and was slowly added to a cold, saturated Na_2CO_3 aqueous solution (ca. 600 mL). The reaction mixture was extracted with diethyl ether (4×200 mL) and the combined organic phases were dried over Na_2SO_4 and concentrated in vacuo to yield a pale-yellow solid crude product, which was evaporated onto silica and purified by flash chromatography (EtOAc/heptane 1:1, 7×6 cm) to afford (*R*,*S*)-**5** as a white solid (7.45 g, >99%). M.p. (*rac*) 98.2–98.8 °C; m.p. (*ee* >99%) 107.8–108.0 °C; $[\alpha]_D^{20}=+334.9$ ($c=0.0129$ in $CHCl_3$); ^{1}H NMR (400 MHz, $CDCl_3$): $\delta=8.06$ (apparent d, 1H $J=8.80$ Hz), 7.92 (s, 1H), 7.76 (apparent d, 1H $J=8.00$ Hz), 7.69 (ddd, 1H $J=1.60$, 7.00, 8.40 Hz), 7.51 (ddd, 1H 1.20, 6.80, 8.00 Hz), 3.56 (bs, 1H), 3.39 (ddd, 1H $J=1.20$, 6.80, 17.70 Hz), 3.02–3.08 (m, 2H), 2.31–2.37 (m, 4H), 2.18–2.26 (m, 1H), 1.91–2.01 ppm (m, 1H); ^{13}C NMR (100 MHz, $CDCl_3$): $\delta=213.56$, 160.21, 147.26, 135.40, 129.27, 128.74, 128.33, 127.64, 127.19, 126.34, 44.75, 37.02, 36.59, 33.90, 31.95, 31.51 ppm; IR (KBr): $\tilde{\nu}=1490$ (m), 1718 (s), 2933 (s), 3049 cm^{-1} (w); elemental analysis (%) calcd for $C_{16}H_{15}NO$: C 80.98, H 6.37, N 5.90; found: C 80.68, H 6.52, N 5.81; HRMS (ESI): *m*/*z*: calcd for $C_{16}H_{16}NO$: 238.1232 [$M+H^+$]; found: 238.1223.

(+)-(8*R*,10*S*,12*R*)-8,12-Methano-10-bromo-9-oxo-cycloocta[5,4-*b*]quinoline ((*R*,*R*)-*exo*-11): A solution of bromine (159 μL, 3.10 mmol) in $CHCl_3$ (9.3 mL) was added dropwise to a solution of (*R*,*S*)-**5** (0.78 g, 3.3 mmol) in $CHCl_3$ (9.3 mL) and trifluoroacetic acid (9.3 mL) at 0 °C. The reaction mixture was stirred at room temperature for 3 h and quenched by the addition of saturated aqueous $NaHCO_3$. The mixture was extracted with EtOAc and the combined organic phases were dried over Na_2SO_4 and concentrated in vacuo. The crude product was evaporated onto celite and purified by flash chromatography (petroleum ether/EtOAc 1:1) followed by recrystallization from $CHCl_3$ to afford (*R*,*R*)-*exo*-**11** (0.81 g, 2.6 mmol, 78%). M.p. 170.2–170.9 °C; $[\alpha]_D^{20}=+205.3$ ($c=0.0142$ in $CHCl_3$); ^{1}H NMR (400 MHz, $CDCl_3$): $\delta=8.07$ (d, 1H $J=8.40$ Hz), 7.95 (s, 1H), 7.77 (d, 1H $J=8.40$ Hz), 7.71 (ddd, 1H $J=1.20$, 7.00, 8.50 Hz), 7.54 (ddd, 1H $J=1.20$, 6.80, 8.00 Hz), 4.30 (dd, 1H $J=6.80$, 13.20 Hz), 3.60 (bs, 1H), 3.37–3.46 (m, 2H), 3.07–3.13 (m, 1H), 2.96 (tdt, 1H $J=3.20$, 6.80, 6.40 Hz), 2.57 (dt, 1H $J=3.80$, 13.00 Hz), 2.38–2.46 ppm (m, 2H); ^{13}C NMR (100 MHz, $CDCl_3$): $\delta=203.24$, 158.52, 147.16, 136.04, 129.77, 128.65, 127.74, 127.24, 127.15, 126.79, 51.81, 46.29, 45.22, 39.53, 31.79, 31.07 ppm; IR (KBr): $\tilde{\nu}=1720$, 1492 cm^{-1}; elemental analysis (%) calcd for $C_{16}H_{14}BrNO\cdot 1/20\,CHCl_3$: C 59.84, H 4.40, N 4.35; found: C 60.09, H 4.76, N 4.27; HRMS (ESI): *m*/*z*: calcd for $C_{16}H_{15}NOBr$: 316.0337 [$M+H]^+$; found: 316.0336.

(8*R*,12*R*)-10-Amino-8,12-methano-9-oxo-cycloocta[5,4-*b*]quinoline ((*R*,*R*)-12): Sodium azide (216 mg, 3.32 mmol) was added to a solution of (*R*,*R*)-*exo*-**11** (1.00 g, 3.16 mmol) in anhydrous DMF (120 mL). The reaction mixture, which turned yellow after approximately 2 min, was stirred for 25 min (100% conversion according to mass spectrometry) before water (100 mL) was added. The reaction mixture was extracted with EtOAc (4×200 mL), and the combined organic phases were washed with water (5×350 mL), dried over Na_2SO_4, and concentrated onto celite. The celite was loaded on a pad of silica and the intermediate enaminoketone (*R*,*R*)-**12** was eluted with EtOAc (522 mg). The enaminoketone turned out to be rather unstable and thus was not rigorously characterised. ^{1}H NMR (400 MHz, $CDCl_3$): $\delta=7.95$ (d, 1H $J=8.80$ Hz), 7.77 (s, 1H), 7.64 (d, 1H $J=8.80$ Hz), 7.58–7.63 (m, 1H), 7.40–7.44 (m, 1H), 6.21 (dd, 1H $J=1.60$, 7.60 Hz), 3.81–3.85 (m, 1H), 3.56 (bs, 2H), 3.29–3.36 (m, 1H), 3.03–3.09 (m, 2H), 2.68–2.73 (m, 1H), 2.27–2.32 ppm (m, 1H); ^{13}C NMR (100 MHz, $CDCl_3$): $\delta=197.54$, 159.57, 146.25 138.96, 137.10, 129.10, 128.31, 127.78, 127.04, 126.88, 126.00, 121.49, 40.31, 38.43, 31.09, 30.45 ppm.

(+)-(8*R*,11*R*,19*R*,22*R*)-8,22:11,19-Dimethanodiquinolino[2,3-*e*:3′,2′-*e*′]pyrazino[2,3-*a*:6,5-*a*′]dicyclooctane ((*R*,*R*,*R*,*R*)-4): EtOAc (130 mL), previously purged with nitrogen, was added to a mixture of Pd/C (10%, 522 mg) and (*R*,*R*)-**12** (522 mg, 2.09 mmol). The reaction mixture was purged with nitrogen for 10 min and hydrogen for 10 min before HOAc (1.3 mL) was added. The reaction mixture was allowed to stir under hydrogen for 3.5 h and under nitrogen overnight. The mixture was filtered through a pad of celite, and the filtrate was reduced to approximately 50 mL in vacuo, washed with saturated aqueous $NaHCO_3$, and concentrated in vacuo. The product was purified in a first step by flash chromatography (5×10 cm; less polar by-products were eluted with CH_2Cl_2 containing 3% MeOH and the product was eluted with 6% MeOH). The concentrated fractions containing (*R*,*R*,*R*,*R*)-**4** were dissolved in the smallest possible amount of CH_2Cl_2 followed by the addition of twice the amount of EtOAc. The solution was concentrated in vacuo until precipitation occurred. The suspension was kept in a fridge overnight to complete the precipitation. The product was collected by filtration with a Pasteur pipette clogged with cotton wool. The product was washed with EtOAc, eluted with CH_2Cl_2, and concentrated in vacuo to yield (*R*,*R*,*R*,*R*)-**4** (160 mg, 0.343 mmol, 16%). M.p. 302 °C (decomp); $[\alpha]_D^{20}=+614.7$ ($c=0.0083$ in $CHCl_3$); ^{1}H NMR (400 MHz, $CDCl_3$, 51.2 mM): $\delta=7.66$ (d, 2H $J=8.40$ Hz, H-2(13)), 7.33 (ddd, 2H $J=1.60$, 6.80, 8.50 Hz, H-3(14)), 7.00 (ddd, 2H $J=1.20$, 7.20, 8.00 Hz, H-4(15)), 6.42 (d, 2H $J=8.40$ Hz, H-5(16)), 5.34 (s, 2H; H-6(17)), 3.46 (bs, 2H; H-11(22), 3.41–3.46 (m, 2H; H-10(21)-*exo*), 3.33 (bs, 2H; H-8(19)), 3.21–3.26 (m, 2H; H-10(21)-*endo*), 2.64–2.73 (m, 4H; H-7(18)), 2.20–2.24 (m, 2H; H-23(24)), 2.05–2.08 ppm (m, 2H; H-23(24)); ^{13}C NMR (100 MHz, $CDCl_3$): $\delta=160.25$ (C-11′(22′)), 153.69 (C-8′(19′)), 148.96 (C-9′(20′)), 146.25 (C-1′-(12′)), 135.56 (C-6(17)), 128.47 (C-3(14)), 127.62 (C-2(13)), 126.40 (C-5′-(16′) or (C-6′(19′)), 126.35 C-5′(16′) or (C-6′(19′)), 126.30 (C-5(16)), 125.32 (C-4(15), 40.81 (C-10(21)), 36.59 (C-7(18)), 36.14 (C-11(22)), 34.57 (C-8(19)), 28.25 ppm (C-23(24)); IR (KBr): $\tilde{\nu}=2938$ (s), 1626, 1600 (m), 1492 cm^{-1}; elemental analysis (%) calcd for $C_{32}H_{26}N_4\cdot 2.5\,H_2O$: C 77.39, H 5.95, N 11.28; found: C 77.02, H 5.98, N 11.23; HRMS (ESI): *m*/*z*: calcd for $C_{32}H_{26}N_4$: 467.2236 [$M+H^+$]; found: 467.2248.

^{1}H NMR spectroscopic dilution titration experiments (for racemic and enantiomerically pure 4): A sample of known concentration (typically 49 mM) was prepared in $CDCl_3$ (400 μL) and a ^{1}H NMR spectra was recorded. $CDCl_3$ (typically 100–300 μL) was sequentially added to the solution. A ^{1}H NMR spectrum was recorded after each addition.

Crystallography: Crystals of *rac*-**4** were obtained by dissolving *rac*-**4** in the minimum amount of CH_2Cl_2, an equal amount of heptane was added, and the mixture was allowed to stand at room temperature. The intensity datasets for *rac*-**4** were collected at 150 K with a MARCCD system using ω scans and synchrotron radiation at MAXLAB II (Lund, Sweden; $\lambda=0.90700$ Å).[53] The CCD data were extracted and integrated by using an X-ray data streamer (XDS).[54] The structure was solved by direct methods and refined by full-matrix least-squares calculations on F^2 by using SHELXL 97.[55] The non-hydrogen atoms were refined with anisotropic displacement parameters. All the hydrogen atoms were constrained to parent sites by using a riding model. The use of synchrotron radiation with a high wavelength gave a $\sin\Theta/\lambda$ value that was too low, but the crystals scattered too weakly to rectify this. CCDC-746931 contains the supplementary crystallographic data for this paper. These data can be obtained free of charge from The Cambridge Crystallographic Data Centre via www.ccdc.cam.ac.uk/data_request/cif

Crystal data and collection and refinement details: $C_{32}H_{26}N_4\cdot 0.5\,CH_2Cl_2$, $M_r=509.03$, monoclinic, $a=14.270(3)$, $b=18.070(4)$, $c=20.260(4)$ Å, $\beta=110.04(3)°$, $V=4908.0(17)$ Å^3, space group $P2_1/n$ (no. 14), $Z=8$, $\mu=0.186$ mm^{-1}, $\rho_{calcd}=1.378$ $g\,cm^{-3}$, $\theta=1.95$–$29.28°$, 83853 reflections measured, 6372 unique ($R_{int}=0.0409$), which were used in all the calculations. The final $wR(F^2)=0.1063$, $S=1.108$ (all data), $R(F)=0.0410$ ($I>2\sigma(I)$).

Acknowledgements

We thank the Swedish Foundation for Strategic Research, The Crafoord Foundation, The Swedish Research Council, and The Royal Physiographic Society (Lund) for financial support. MAXLAB in Lund is acknowledged for beam time.

[1] J. W. Steed, J. L. Atwood, *Supramolecular Chemistry*, 2nd ed., Wiley, Chichester, **2009**, Chapter 3–6.
[2] C. W. Chen, H. W. Whitlock, *J. Am. Chem. Soc.* **1978**, *100*, 4921–4922.
[3] S. C. Zimmerman, C. M. Vanzyl, *J. Am. Chem. Soc.* **1987**, *109*, 7894–7896.
[4] M. Harmata, *Acc. Chem. Res.* **2004**, *37*, 862–873.
[5] J. W. Steed, J. L. Atwood in *Encyclopedia of Supramolecular Chemistry*, (Eds.: J. W. S. Jerry, L. Atwood), CRC, **2004**, p. 1744.
[6] Z. G. Wang, B. H. Zhou, Y. F. Chen, G. D. Yin, Y. T. Li, A. X. Wu, L. Isaacs, *J. Org. Chem.* **2006**, *71*, 4502–4508.
[7] P. Polavarapu, H. Melander, V. Langer, A. Gogoll, H. Grennberg, *New J. Chem.* **2008**, *32*, 643–651.
[8] F. G. Klärner, M. Lobert, U. Naatz, H. Bandmann, R. Boese, *Chem. Eur. J.* **2003**, *9*, 5036–5047.
[9] M. Havlik, V. Král, R. Kaplánek, B. Dolenský, *Org. Lett.* **2008**, *10*, 4767–4769.
[10] a) A. Hansson, T. Wixe, K.-E. Bergquist, K. Wärnmark, *Org. Lett.* **2005**, *7*, 2019–2022; b) J. Artacho, J. Nilsson, K.-E. Bergquist, O. F. Wendt, K. Wärnmark, *Chem. Eur. J.* **2006**, *12*, 2692–2701.
[11] B. Branchi, V. Balzani, P. Ceroni, M. C. Kuchenbrandt, F. G. Klärner, D. Blaser, R. Boeso, *J. Org. Chem.* **2008**, *73*, 5839–5851.
[12] S. C. Zimmerman, C. M. Vanzyl, G. S. Hamilton, *J. Am. Chem. Soc.* **1989**, *111*, 1373–1381.
[13] P. Artacho, J. Nilsson, K.-E. Bergquist, O. F. Wendt, K. Wärnmark, *Chem. Eur. J.* **2006**, *12*, 2692–2701.
[14] X. X. Peng, H. Y. Lu, T. Han, C. F. Chen, *Org. Lett.* **2007**, *9*, 895–898.
[15] A. Lohr, M. Grune, F. Wurthner, *Chem. Eur. J.* **2009**, *15*, 3691–3705.
[16] F. C. Krebs, M. Jorgensen, *J. Org. Chem.* **2001**, *66*, 6169–6173.
[17] H. Iwamoto, Y. Hidaka, Y. Fukazawa, *Tetrahedron Lett.* **2008**, *49*, 277–280.
[18] B. W. Greenland, S. Burattini, W. Hayes, H. M. Colquhoun, *Tetrahedron* **2008**, *64*, 8346–8354.
[19] V. A. Azov, R. Gomez, J. Stelten, *Tetrahedron* **2008**, *64*, 1909–1917.
[20] T. Nishiuchi, Y. Kuwatani, T. Nishinaga, M. Iyoda, *Chem. Eur. J.* **2009**, *15*, 6838–6847.
[21] A. Petitjean, R. G. Khoury, N. Kyritsakas, J. M. Lehn, *J. Am. Chem. Soc.* **2004**, *126*, 6637–6647.
[22] D. J. Feng, G. T. Wang, J. Wu, R. X. Wang, Z. T. Li, *Tetrahedron Lett.* **2007**, *48*, 6181–6185.
[23] A. M. M. Abe, J. Helaja, A. M. P. Koskinen, *Org. Lett.* **2006**, *8*, 4537–4540.
[24] T. H. Kwon, K. S. Jeong, *Tetrahedron Lett.* **2006**, *47*, 8539–8541.
[25] J. M. Hermida-Ramon, C. M. Estevez, *Chem. Eur. J.* **2007**, *13*, 4743–4749.
[26] S. C. Zimmerman, W. M. Wu, *J. Am. Chem. Soc.* **1989**, *111*, 8054–8055.
[27] L. J. Dsouza, U. Maitra, *J. Org. Chem.* **1996**, *61*, 9494–9502.
[28] B. Legouin, P. Uriac, S. Tomasi, L. Toupet, A. Bondon, P. van de Weghe, *Org. Lett.* **2009**, *11*, 745–748.
[29] G. Fukuhara, S. Madenci, J. Polkowska, F. Bastkowski, F. G. Klärner, Y. Origane, M. Kaneda, T. Mori, T. Wada, Y. Inoue, *Chem. Eur. J.* **2007**, *13*, 2473–2479.
[30] C. Pardo, E. Sesmilo, E. Gutierrez-Puebla, A. Monge, J. Elguero, A. Fruchier, *J. Org. Chem.* **2001**, *66*, 1607–1611.
[31] J. Fleischhauer, M. Harmata, M. Kahraman, A. Koslowski, C. J. Welch, *Tetrahedron Lett.* **1997**, *38*, 8655–8658.
[32] S. Sergeyev, S. Stas, A. Remacle, C. Velde, B. Dolenský, M. Havlík, V. Král, J. Čejka, *Tetrahedron: Asymmetry* **2009**, *20*, 1918–1923.
[33] C. J. Wallentin, E. Orentas, E. Butkus, K. Wärnmark, *Synthesis* **2009**, 864–867.
[34] K. Naemura, T. Matsumura, M. Komatsu, Y. Hirose, H. Chikamatsu, *Bull. Chem. Soc. Jpn.* **1989**, *62*, 3523–3530.
[35] K. Naemura, T. Matsumura, M. Komatsu, Y. Hirose, H. Chikamatsu, *J. Chem. Soc. Chem. Commun.* **1988**, 239–241.
[36] S. Stončius, E. Orentas, E. Butkus, L. Öhrström, O. F. Wendt, K. Wärnmark, *J. Am. Chem. Soc.* **2006**, *128*, 8272–8285.
[37] S. Stončius, E. Butkus, A. Zilinskas, K. Larsson, L. Öhrström, U. Berg, K. Wärnmark, *J. Org. Chem.* **2004**, *69*, 5196–5203.
[38] C. Marjo, R. Bishop, *Eur. J. Org. Chem.* **2001**, 863–873.
[39] C.-J. Wallentin, E. Orentas, M. T. Johnson, E. Butkus, O. F. Wendt, L. Öhrström, K. Wärnmark, *CrystEngComm* **2009**, *11*, 1837–1841.
[40] S. C. Zimmerman, M. Mrksich, M. Baloga, *J. Am. Chem. Soc.* **1989**, *111*, 8528–8530.
[41] T. Momose, E. Yoshizawa, O. Muraoka, *Synth. Commun.* **1985**, *15*, 17–25.
[42] M. C. Wani, A. W. Nicholas, G. Manikumar, M. E. Wall, *J. Med. Chem.* **1987**, *30*, 1774–1779.
[43] C. E. Marjo, M. L. Scudder, D. C. Craig, R. Bishop, *J. Chem. Soc. Perkin Trans. 2* **1997**, 2099–2104.
[44] T. L. Ho, E. Gorobets, *Tetrahedron* **2002**, *58*, 4969–4973.
[45] M. Drögemüller, T. Flessner, R. Jautelat, U. Scholz, E. Winterfeldt, *Eur. J. Org. Chem.* **1998**, 2811–2831.
[46] K. Brandenburg, DIAMOND, Program for Molecular Graphics Crystal Impact, Bonn, Germany, **2000**.
[47] R. Bishop in *Enantiomer Ordering and Separation during Molecular Inclusion in Separations and Reactions in Supramolecular Chemistry* (Eds.: F. Toda, R. Bishop), Wiley, Chichester, **2004**, Chapter 2, pp. 33–60.
[48] I. Horman, B. Dreux, *Helv. Chim. Acta* **1984**, *67*, 754–764.
[49] A. P. Bisson, C. A. Hunter, J. C. Morales, K. Young, *Chem. Eur. J.* **1998**, *4*, 845–851.
[50] H. Adams, C. A. Hunter, K. Lawson, J. Perkins, S. E. Spey, C. J. Urch, J. M. Sanderson, *Chem. Eur. J.* **2001**, *7*, 4863–4878.
[51] Y. Nakao, H. Sugeta, Y. Kyogoku, *Bull. Chem. Soc. Jpn.* **1985**, *58*, 1767–1771.
[52] S. Ghosh, A. X. Wu, J. C. Fettinger, P. Y. Zavalij, L. Isaacs, *J. Org. Chem.* **2008**, *73*, 5915–5925.
[53] C. B. Mammen, T. Ursby, M. Thunnissen, J. Als-Nielsen, *AIP Conf. Proc.* **2004**, *705*, 808–811.
[54] W. J. Kabsch, *Appl. Crystallogr.* **1993**, *26*, 795–800.
[55] G. M. Sheldrick, *Acta Crystallogr. Sect. A* **2008**, *64*, 112–122.

Received: October 22, 2009
Published online: February 24, 2010

